AD658383

CF-2915
25 January 1961
COPY NO. 111

THEORETICAL ANALYSIS OF PLASMA CONFINEMENT IN A ROTATING MAGNETIC FIELD

by

D. K. Taylor

THE JOHNS HOPKINS UNIVERSITY
APPLIED PHYSICS LABORATORY
8621 GEORGIA AVENUE SILVER SPRING, MARYLAND

Operating under Contract NOrd 7386 with the Bureau of Naval Weapons, Department of the Navy

32

THE JOHNS HOPKINS UNIVERSITY
APPLIED PHYSICS LABORATORY
SILVER SPRING MARYLAND

THEORETICAL ANALYSIS OF PLASMA CONFINEMENT IN A ROTATING MAGNETIC FIELD

by

D. K. Taylor

Table of Contents

Foreword

The physical reasoning which led to the conclusion by the author that particle trajectories in a rotating field are stable in the plane of rotation functions as an introduction to the reader of the concept of plasma confinement in a rotating field.

The magnetic field's relation to Maxwell's equations is discussed and the induced electric field is presented, whereupon the equations of motion and their exact general solutions are given.

The orbits of particles are derived for special limiting cases on the basis of the general solutions, and the orbits are compared with the analog computer solutions of the equations.

It is shown that a rotating magnetic field alone is not enough to confine a plasma* but that the rotating field used in conjuction with other types of stationary fields should result in an effective plasma containment device.

Finally, two additional, physically-possible rotating fields are introduced and their properties are discussed briefly.

I. Orientation

Interest in plasma physics has grown exponentially during the last decade; and during that time, many confinement devices have been proposed and some tested, but none were sufficient for confining that all-important substance—the thermonuclear plasma. All of the confinement devices to date have had a common fault: particle leakage.

The basic method for confining a plasma, which is considered by some to be the only possible way, is to trap it in a magnetic field. A major problem in plasma physics, therefore, is the design of a magnetic field which has minimal particle leakage.

This paper describes another leaky field configuration, but there exists a possible application of the proposed device such that the leakage is acceptable (see Section VI).

II. Introduction to the Rotating Field Concept.

The reasoning which led to the conception of a rotating field for confining plasmas proceeded as follows:

---

* Confinement is achieved in the plane of rotation but not always in the direction normal to the plane of rotation.

(a) (b)

Figure 1 - Stepwise Rotating Magnetic Field.

A particle spirals in a uniform magnetic field as in Figure 1(a). Hence, a particle would escape from a uniform field of finite dimensions. Suppose now the field in Figure 1(a) is suddenly replaced by the perpendicular field in Figure 1(b). The original component of axial velocity is converted to azimuthal velocity and vice versa, so the particle is again moving along lines of force. If the field-rotation process is continued in this stepwise manner, some of the particle should possess orbits as shown in Figure 2(a).

(a) (b)

Figure 2 - Particle Orbit in a Stepwise Rotating Magnetic Field.

But some particles, because their velocities are in the wrong direction at the instant the field changes, will possess orbits as in Figure 2(b).

This clearly reveals the fact that particles tend to follow lines of force as they rotate. Consider, now, a magnetic field rotating with a uniform angular frequency ω_0. If ω_0 is slightly smaller than the frequency of rotation ω_L (Larmor frequency) of the particle in the field, then the particle obviously spirals as in Figure 3.

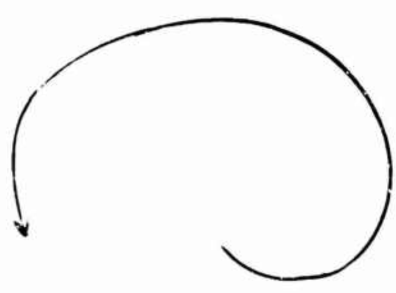

Figure 3 - Spiraling Orbit in Rotating Magnetic Field with $\omega_0 < \omega_L$.

But, if ω_o is greater than ω_L, a particle is turned by the field quicker than it can move along a field line and is therefore bounded within the plane of rotation.

This, therefore, implies the following confinement conditions:

(i) $\omega_o < \omega_L$: Particles are unconfined in the plane of rotation

(ii) $\omega_o > \omega_L$: Particles are confined in the plane of rotation.

$\omega_o = \omega_L$ is called, hereafter, the critical frequency.

In the confined state, most particles are however unconfined in the direction normal to the plane of rotation. This may be realized by considering a particle which is instantaneously moving upward in a field with $\omega_o > \omega_L$. In one xy-plane* orbit, the particle will not have time to complete a Larmor orbit (since $\omega_o > \omega_L$); and hence, after one period, the particle is still moving upward. Hence, the particle is unconfined in the z-direction. The exact condition for confinement in the z-direction will be derived later.

III. Fields

The rotating magnetic field, illustrated with respect to an xy-coordinate system in Figure 4, is desired to have the form of Equation (1) for non-relativistic rotation.

$$\underline{B} = B_o \left[\underline{i} \sin \omega_o t + \underline{j} \cos \omega_o t\right] \qquad (1)$$

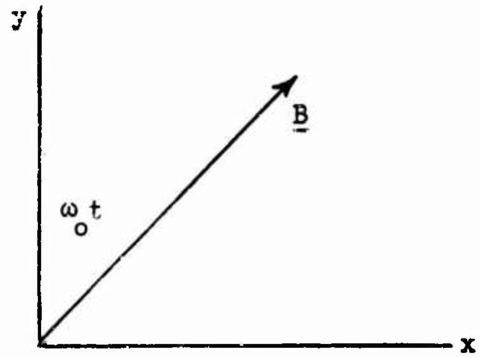

The magnitude of the field is the constant B_o. Hence, Equation (1) represents a uniform rotating field.

FIGURE 4. Coordinate System.

A necessary condition for $\underline{B}$ to be a physically possible field is for it to satisfy the wave equation:

$$\nabla^2 \underline{B} = \frac{1}{c^2} \frac{\partial^2 \underline{B}}{\partial t^2} \; . \qquad (2)$$

*See Figure 4.

Substitution shows that Equation (1) is not a solution of Equation (2), which means that a uniform rotating field cannot exist. However, it is proven in Appendix 1 that Equation (1) represents an approximate solution of Equation (2), the approximation being valid for small frequency-distance products.

The exact expression for the rotating field is derived in Appendix 1 as

$$\underline{B} = B_o \left[\underline{i} \cos \sigma y \sin \omega_o t + \underline{j} \cos \sigma x \cos \omega_o t \right] \tag{3}$$

where $\sigma = \frac{\omega_o}{c}$.

As σy and $\sigma x \rightarrow 0$, Equation (3) reduces to Equation (1).

The size of field necessary to contain a one hundred million degree plasma, given by the condition that the magnetic pressure

$$P_m = B^2/8\Pi$$

exceeds the plasma pressure

$$P_p = nkT,$$

is on the order of 30kG. It is presently beyond the state of the art to construct a 30kG field which rotates at the Larmor frequency; but, as discussed in Section VI, large rotating fields may not be necessary. It is proposed that a small rotating field can be superimposed on a large stationary field, resulting in a practical device.

The vector potential, defined by the equation

$$\underline{B} = \nabla \times \underline{A} , \tag{4}$$

is given by

$$\underline{A} = B_o \left[y \sin \omega_o t - x \cos \omega_o t \right] \underline{k} \tag{5}$$

for the approximate field. The induced electric field is calculated by substituting Equation (5) in Faraday's law:

$$\underline{E} = - \frac{1}{c} \frac{\partial \underline{A}}{\partial t} \tag{6}$$

The resulting expression is:

$$\underline{E} = -\frac{\omega_o B_o}{c} [y \cos \omega_o t + x \sin \omega_o t]. \qquad (7)$$

The exact expression for $\underline{E}$, consistent with Equation (3), is given by the following:

$$\underline{E} = - B_o \, [\sin \sigma y \cos \omega_o t + \sin \sigma x \sin \omega_o t] \, \underline{k} \qquad (7a)$$

Equation's (1) and (7) are the field equations which enter into the equations of motion derived in the next section. The simplified field expressions lead to differential equations which have exact solutions, and they are fairly accurate for $\omega_o \sim \omega_L$.

Both field's (1) and (3) contain another approximation which is not quite correct. It was assumed that $v/c \ll 1$ at every point in space where v is the speed of the field with respect to inertial space, which is obviously a bad assumption for high frequencies of rotation or for large distances from the origin. Calculation shows, however, that the approximation is fair for $\omega_o/\omega_L < 10$ and $\sqrt{x^2+y^2} < 10$. For small frequency-distance products, the relativistic field expressions reduce to Equations (1) and (7). All statements in this paragraph are proven in Appendix 2.

IV. Equations of Motion of a Charged Particle in an Electromagnetic Field.

(a) Laboratory Coordinates

The equation of motion of a particle with charge q and mass m in a magnetic field $\underline{B}$ and an electric field $\underline{E}$ is obtained by applying the Lorentz force equation to Newton's second law. The vector equation of motion is:

$$m \frac{d\underline{V}}{dt} = q \left[\underline{E} + \frac{1}{c} \underline{V} \times \underline{B}\right] \qquad (8)$$

Using the expression for $\underline{E}$ derived in the previous section, the component equations are immediately written as:

$$\begin{aligned} m\dot{V}_x &= -\frac{qB}{c} V_z \cos \omega_o t \\ m\dot{V}_y &= \frac{qB}{c} V_z \sin \omega_o t \qquad (9) \\ m\dot{V}_z &= -\frac{qB}{c} (y\omega_o \cos \omega_o t + x\omega_o \sin \omega_o t) + \frac{qB}{c} (V_x \cos \omega_o t - V_y \sin \omega_o t) \end{aligned}$$

where:

$$\left.\begin{aligned} \dot{x} &= V_x \\ \dot{y} &= V_y \\ \dot{z} &= V_z \end{aligned}\right\} \qquad (10)$$

Equations (9) are relatively complicated and their solutions are not immediately apparent. It is clear, however, that the sines and cosines are introduced by the rotating field, and therefore transforming to a rotating reference frame should remove these factors and simplify the equations considerably. This indeed happens under such a transformation.

(b) Rotating Coordinates

A rotating reference frame is choosen, as illustrated in Figure 5, according to the orthogonal transformation:

$$\begin{pmatrix} x \\ y \end{pmatrix} = \begin{pmatrix} \sin \omega_o t & -\cos \omega_o t \\ \cos \omega_o t & \sin \omega_o t \end{pmatrix} \begin{pmatrix} X \\ Y \end{pmatrix} \qquad (11)$$

where X and Y are rotating coordinates.

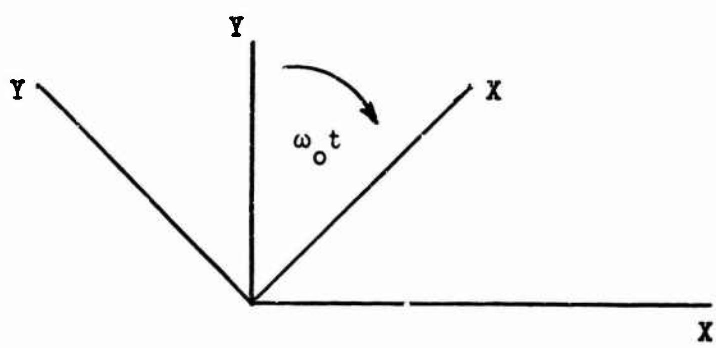

FIGURE 5.

The transformed equations are:

$$\left.\begin{aligned} \ddot{X} &= -2\omega_o \dot{Y} + \omega_o^2 X \\ \ddot{Y} &= +2\omega_o \dot{X} + \omega_o^2 Y + \omega_L V_Z \\ \dot{V}_Z &= -\omega_L \dot{Y} \end{aligned}\right\} \qquad (12)$$

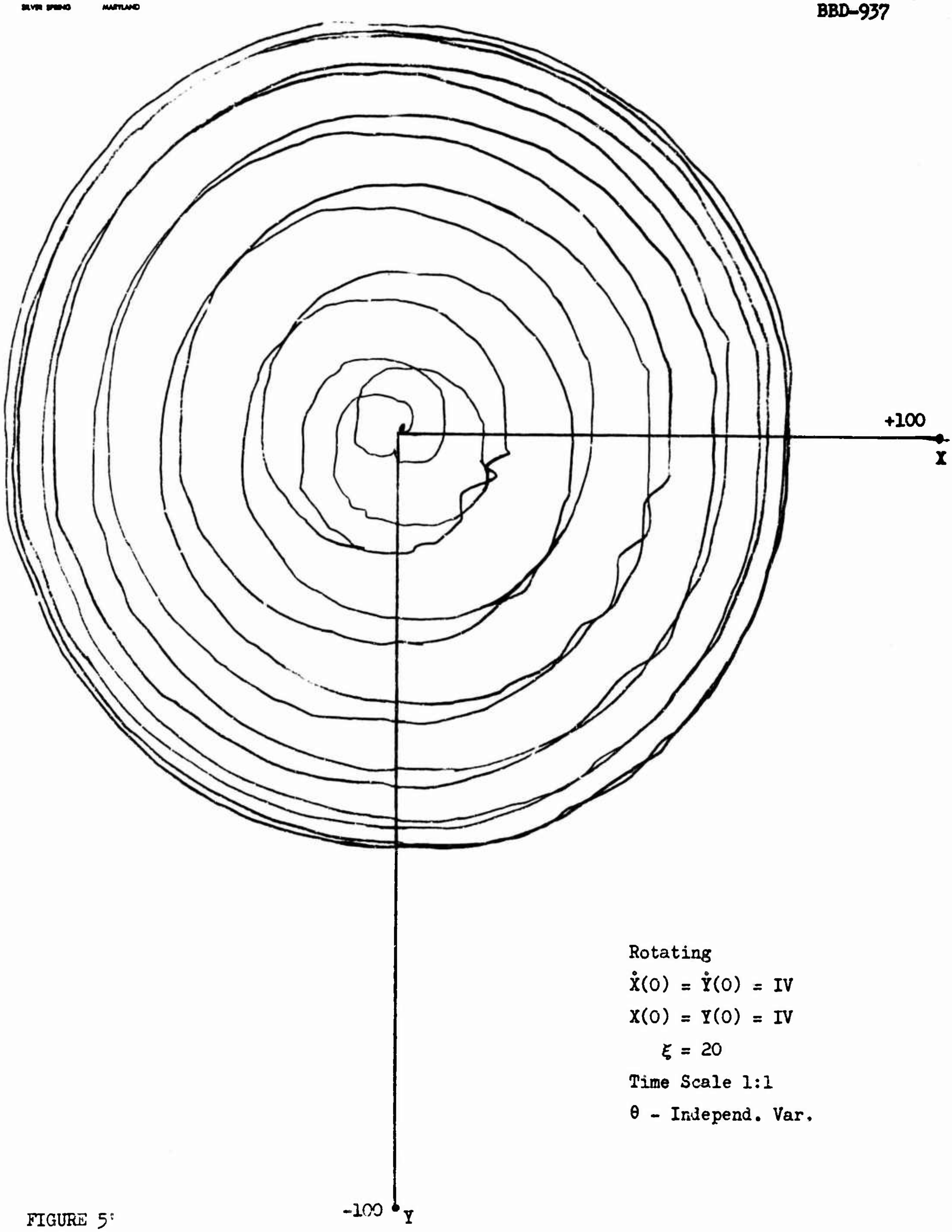

Rotating

$\mathring{X}(0) = \mathring{Y}(0) = IV$

$X(0) = Y(0) = IV$

$\xi = 20$

Time Scale 1:1

θ - Independ. Var.

FIGURE 5

where $z = Z$.

(c) Time Scale Transformation

Equation (12) may be represented more simply, parametrically, if one defines

$$\xi = \frac{\omega_o}{\omega_L} \tag{13}$$

and transforms the time scale according to

$$\omega_o t = \xi \tau . \tag{14}$$

The resulting equations in rotating coordinates are

$$\left.\begin{aligned} \frac{d^2X}{d\tau^2} &= -\,2\xi \frac{dY}{d\tau} + \xi^2 X \\ \frac{d^2Y}{d\tau^2} &= \quad 2\xi \frac{dX}{d\tau} + \xi^2 Y + \xi \frac{dZ}{d\tau} \\ \frac{d^2Z}{d\tau^2} &= -\,\frac{1}{\xi}\frac{dY}{d\tau} \end{aligned}\right\} \tag{15}$$

The equations in laboratory coordinates with transformed time scale are:

$$\left.\begin{aligned} \frac{d^2x}{d\tau^2} &= -\,V_z \cos \xi\tau \\ \frac{d^2y}{d\tau^2} &= \quad V_z \sin \xi\tau \\ \frac{d^2z}{d\tau^2} &= -\,\xi\,(y \cos \xi\tau + x \sin \xi\tau) + V_x \cos \xi\tau - V_y \sin \xi\tau \end{aligned}\right\} \tag{16}$$

V. Solution of the Equations of Motion.

The equations of motion will be solved exactly, and solutions corresponding to particular initial conditions will be given as calculated by hand or, in the case of more complicated solutions, as calculated from the differential equations by the analog computer.

First, solutions will be obtained for the simpler equations in rotating coordinates. Then, the solutions will be transformed back to laboratory coordinates.

Equations twelve are given in operator notation as the following matrix equation:

$$\begin{pmatrix} D^2 - \xi^2 & 2\xi D & 0 \\ -2\xi D & D^2 - \xi^2 & -D \\ 0 & D & D^2 \end{pmatrix} \begin{pmatrix} X \\ Y \\ Z \end{pmatrix} = 0 \qquad (17)$$

The solutions are of the form $e^{D\tau}$ where the D's are solutions to the characteristic determinant,

$$\begin{vmatrix} D^2 - \xi^2 & 2\xi D & 0 \\ -2\xi D & D^2 - \xi^2 & -D \\ 0 & D & D^2 \end{vmatrix} = 0 \qquad (18)$$

(a) Critical Frequency

The solutions to Equation (18) provide the critical frequency for confinement which was discussed in Section II. Equation (18) reduces to the sixth order polynomial equation:

$$D^2 \left[D^4 + (2\xi^2+1)\, D^2 + \xi^4 - \xi^2\right] = 0 \qquad (19)$$

The first factor yields a double root D = 0 which corresponds to solutions of the form constant and τ. It will be seen, later, that an expression of the form τ occurs in the Z-solution only. Hence, the stability of the X and Y solutions depends on the second factor of Equation (19). This provides the four roots:

$$D = \pm j \sqrt{\frac{1 + 2\xi^2 \pm \sqrt{1+8\xi^2}}{2}}\ . \qquad (20)$$

Solutions are stable when

$$1 + 2\xi^2 \pm \sqrt{1 + 8\xi^2} > 0, \tag{21}$$

which implies that $\xi \geq 1$. This is equivalent to the critical frequency statement:

$$\omega_o > \omega_L$$

(b) Solutions in Rotating Coordinates

(i) Stable Solution

Define

$$\omega_1 = \sqrt{\frac{1 + 2\xi^2 + \sqrt{1+8\xi^2}}{2}} \tag{22}$$

and

$$\omega_2 = \sqrt{\frac{1 + 2\xi^2 - \sqrt{1+8\xi^2}}{2}} \tag{23}$$

Then, for $\xi > 1$, solutions are linear forms which include only the expressions:

$$\text{constant}, \ \tau, \ e^{\pm j\omega_1\tau} \text{ and } e^{\pm j\omega_2\tau}.$$

Substitution of the linear forms into the equations of motion determines the relations among constants, and, by using Euler's identity,

$$e^{\pm j\varphi} = \cos\varphi \pm j\sin\varphi \ , \tag{24}$$

the general solution in sine-cosine form is obtained. The general stable solution in rotating coordinates is therefore

$$X = \sum_{i=1}^{2} \left[\frac{\omega_i^2+\xi^2-1}{2\xi\omega_i}\right] B_i \cos(\omega_i\tau + \alpha_i) \tag{25}$$

$$Y = \sum_{i=1}^{2} B_i \sin(\omega_i\tau + \alpha_i) + C \tag{26}$$

$$Z = \sum_{i=1}^{2} \frac{B_i}{\omega_i} \cos(\omega_i\tau + \alpha_i) - \xi^2 C\tau + D \tag{27}$$

where α_i, B_i, C and D are arbitrary constants.

The character of orbits can be derived directly from the general solution. For $\xi > 10$, calculation shows that

$$\frac{\omega_i^2 + \xi^2 - 1}{2\xi\omega} \sim 1,$$

which implies that the orbits are of the form:

$$\left(\frac{x}{r}\right)^2 + \left(\frac{y}{r}\right)^2 = 1 + e \cos\left[(\omega_1-\omega_2)\tau + (\alpha_1-\alpha_2)\right] \qquad (28)$$

where $r = \sqrt{B_1^2 + B_2^2}$

and $e = \dfrac{2B_1B_2}{B_1^2+B_2^2}$.

The orbits for $\xi > 10$ are, therefore, circles whose radii oscillate with the angular frequency $(\omega_1-\omega_2)$. For $\xi < 10$, examination of the equations shows that the orbits are slightly elliptical and the oscillation of their radii is not purely sinusoidal. As $\xi\to\infty$, the orbits are circles whose radii oscilates with the angular frequency $\sqrt{2}$.

It follows that there are $(\xi/(\omega_1-\omega_2)^2)$ orbits in one oscillation. This fact is illustrated in the sample orbit, shown in Figure 9, which was plotted by the analog computer.

The z-motion consists of stable oscillations superimposed upon a constant drift velocity V_{zD} given by

$$V_{zD} = -\xi^2 C. \qquad (29)$$

The constant C is given in terms of initial conditions by

$$C = \frac{Y_o + \left(\frac{dZ}{d\tau}\right)_o}{1 - \xi^2} . \qquad (30)$$

Figure 6 shows a sample plot of the z-motion and the corresponding x and y motion for $C \neq 0$. Figure 7 shows z-motion and the corresponding x and y motion for $C = 0$.

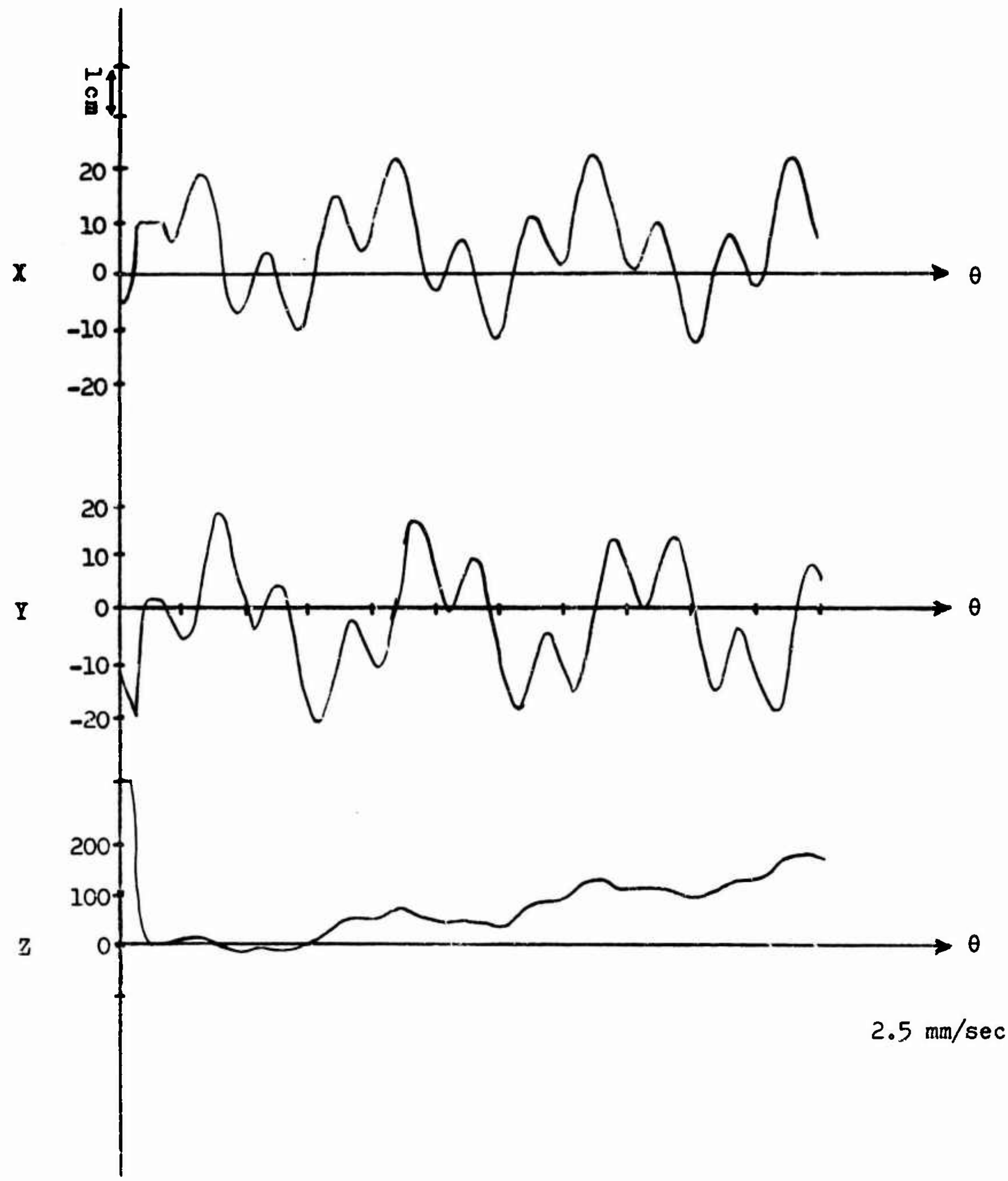

$$\xi = 4$$

$$\left(\frac{dX}{d\theta}\right)_o = -10 \text{ cm}$$

$$\left(\frac{dY}{d\theta}\right)_o = -1 \text{ cm}$$

FIGURE 6.

$$X_o = 5 \text{ cm}$$

$$Y_o = 2 \text{ cm}$$

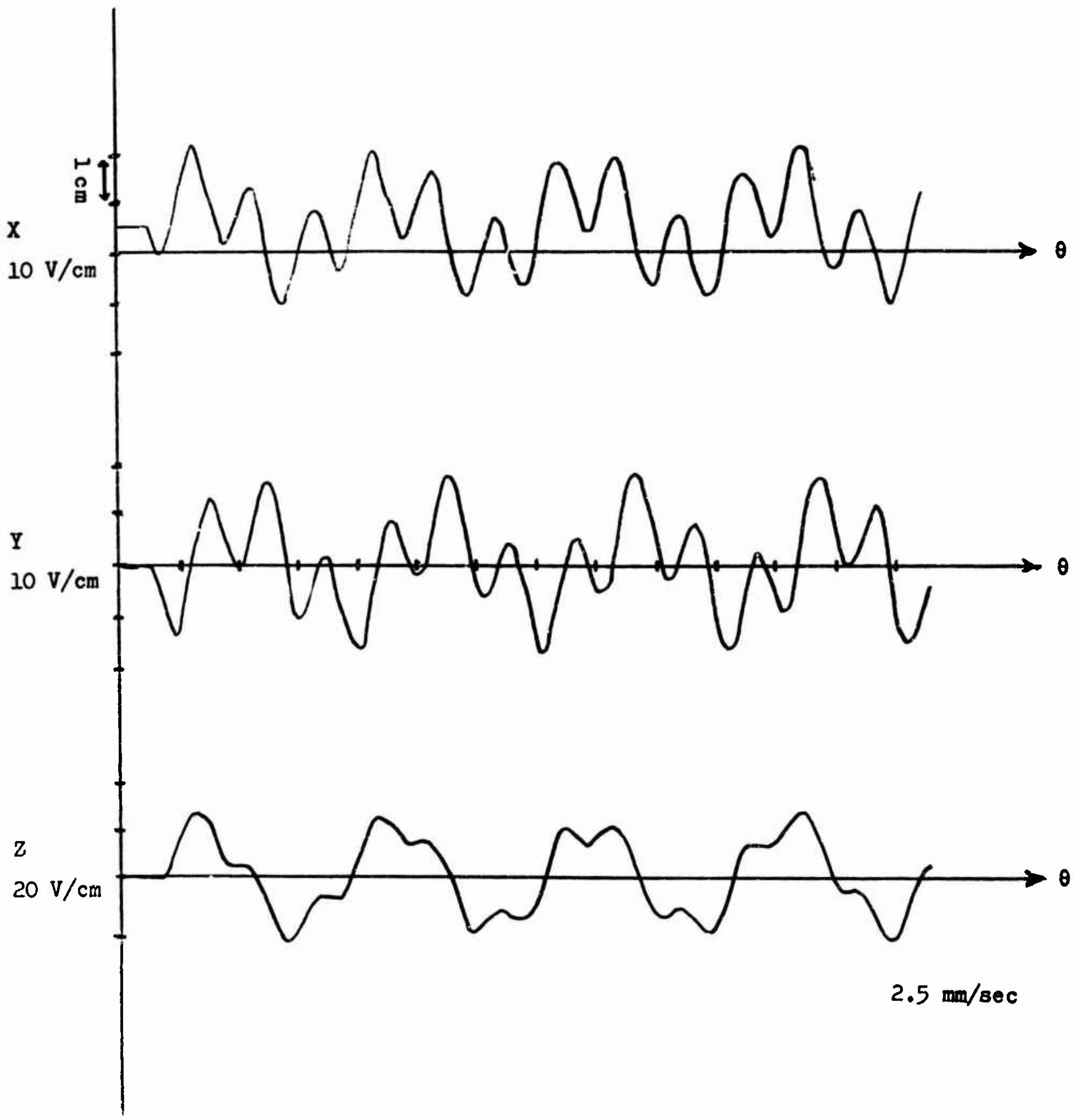

$\xi = 4$

FIGURE 7.

$\dot{x}_o = 10V$

The time scale in the figures is represented by the variable θ given by

$$\theta = \xi\tau \tag{31}$$

where τ is defined by Equation (14).

Equation (29) and (31) are combined to give an explicit expression for drift velocity in terms of initial conditions:

$$V_{zD} = \frac{Y_o + \left(\frac{dZ}{d\tau}\right)_o}{1 - \frac{1}{\xi^2}}$$

or

$$V_{zD} = \frac{\omega_L Y_o + \dot{Z}_o}{1 - \frac{1}{\xi^2}} \text{ in real time.}$$

Calculation on the basis of the above equation shows that a particle, after a collision, will escape at rates on the order of 10^9cm/sec.

This implies that a rotating magnetic field alone is unsuitable for confining a thermonuclear plasma; but, as developed later in Section VI, the rotating field will have important applications to other plasma devices. Figures 5, 6, and 7 clearly illustrate the xy-stability.

(ii) Unstable Solution

Define $a_i = j\omega_i \qquad (i = 1, 2),$ (32)

then the a_i's are real numbers, and the rotating solutions are linear forms which consist in linear combinations of the expression constant, τ, $e^{\pm a_1\tau}$ and $e^{\pm a_2\tau}$. The linear forms can be expressed in terms of hyperbolic functions, time and additive constants.

The general xy-unstable solutions are given by:

$$X = \sum_{i=1}^{2} \alpha_i K_i \sinh (a_i\tau + \beta_i) \tag{33}$$

$$Y = \sum_{i=1}^{2} K_i \cosh (a_i\tau + \beta_i) + C \tag{34}$$

$$Z = -\sum_{i=1}^{2} \frac{K_i}{a_i} \sinh (a_i\tau + \beta_i) - \xi^2 C\tau + D \tag{35}$$

where
$$\alpha_i = \frac{a_i^2 - \xi^2 + 1}{2\xi a_i} \tag{36}$$

and K_i, β_i, C and D are arbitrary constants.

Figure 8 illustrates an XY-unstable solution.

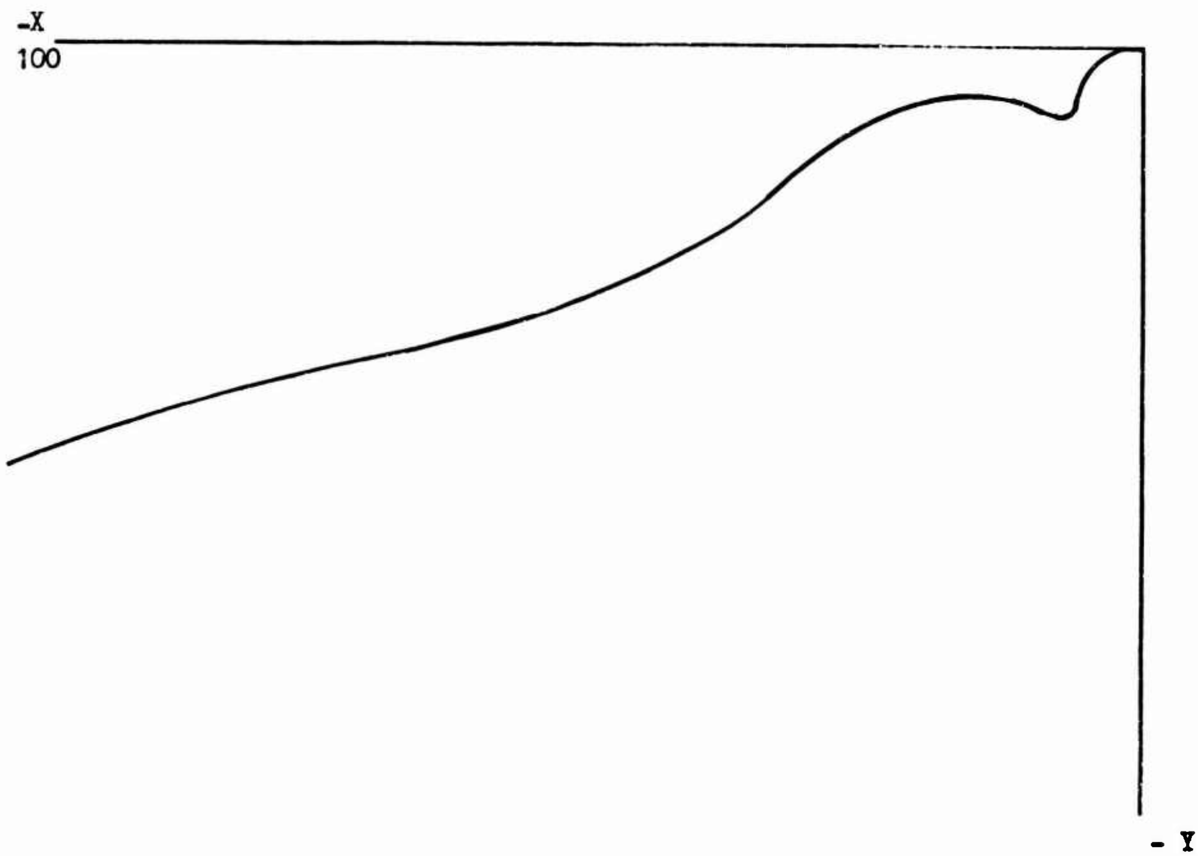

FIGURE 8.

$\xi = .5$

$\frac{dX_o}{d\tau} = -5cm$

(c) Solution in Laboratory Coordinates

The general solution in laboratory coordinates is derived by applying Equations (11) and (14) to Equations (25), (26), and (27). The result is:

$$x = \sum_{i=1}^{2} \left[\frac{\omega_i^2+\xi^2-1}{2\xi\omega_i}\right] B_i \sin \xi\tau \cos (\omega_i\tau+\alpha_i) - B_i \cos \xi\tau \sin (\omega_i\tau+\alpha_i) - C \cos \xi\tau \tag{37}$$

$$y = \sum_{i=1}^{2} B_i \sin \xi\tau \sin (\omega_i\tau+\alpha_i) + \left[\frac{\omega_i^2+\xi^2-1}{2\xi\omega_i}\right] B_i \cos \xi\tau \cos (\omega_i\tau+\alpha_i) + C \sin \xi\tau \tag{38}$$

$$z = \sum_{i=1}^{2} \frac{B_i}{\omega_i} \cos (\omega_i\tau+\alpha_i) - \xi^2 C\tau + D. \tag{39}$$

As $\xi\to\infty$, the coefficients in square brackets approach 1, $C\to 0$, and $(\xi-\omega_1) \to (\xi-\omega_2) \to 1/\sqrt{2}$, which gives the limiting solution

$$x = G_1 \sin (\frac{1}{\sqrt{2}}\tau + \gamma_1) \tag{40}$$

$$y = G_2 \cos (\frac{1}{\sqrt{2}}\tau + \gamma_2). \tag{41}$$

Equations (40) and (41) may be combined to give the equation of the path in the xy-plane:

$$\frac{x^2}{G_1^2} + \frac{y^2}{G_2^2} - \frac{2xy}{G_1G_2} \cos (\gamma_1-\gamma_2) = \sin^2 (\gamma_1-\gamma_2) \tag{42}$$

The above is the equation of an ellipse. If $\gamma-\gamma_2 = \frac{\Pi}{2}$ and $G_1 = G_2$, the orbit is circular. It is interesting that the sense of the orbital angular momentum vector is only a function of the initial conditions, and it does not tend to line up with the vector of the rotating field.

The path in inertial space corresponding to Figure 5 is an ellipse with

$$G_1 = 56.6 \text{ cm}$$

$$G_2 = 1 \text{ cm}$$

$$\gamma_1 = -1°1'$$

$$\gamma_2 = 90°.$$

The computer solution (Figure 9) gave corresponding results for the first half orbit; but by that time, the ellipse had rotated in the $-\omega_o$ direction. This rotation was removed from the idealized elliptical orbit when it was assumed that $\xi \to \infty$. For the orbit in Figure 9, ξ was 20—considerably less than infinity.

The effect of including C (Equations (37)-(39)) in the solution is to superimpose on the ellipse a small amplitude wiggle with frequency ξ. Since C varies as ξ^{-2}, the effect is negligible at high frequency; but the wiggle was visible on computer runs for $\xi \leq 5$.

The revolution frequencies of the particle were checked in both coordinates systems on the analog computer and were found in excellent agreement with those predicted in the general solutions. The oscillation frequency of the orbit in rotating coordinates also checked. These important frequencies in radians per second are listed here:

Angular frequency of revolution in lab coordinates = $\omega_L/\sqrt{2}$

Angular frequency of revolution in rotating coordinates $\approx \omega_o$

Oscillation frequency of orbit in rotating coordinates = $\sqrt{2}\,\omega_L$

VI. Applications of the Rotating Field.

(a) Properties of the Rotating Field

The following are properties of the rotating magnetic field, revealed in the computer solutions of the equations of motion, which suggest possible applications of rotating magnetic fields to other existing plasma confinement devices:

A. All particles possess stable motion in planes parallel to the plane of field rotation when the angular frequency of field rotation ω_o exceeds the Larmor frequency of the particle ω_L.

B. Linear motion of a particle in a rotating field is partially transformed into azimuthal motion.

C. Motion in the direction normal to the plane of rotation consists in a constant drift superimposed on a stable oscillatory component.

(b) Suggested Applications

The rotating field has obvious applications to the following three devices, each of which will be discussed in some detail:

A. The Cusped Geometry
B. The Magnetic Mirror
C. The Stellerator

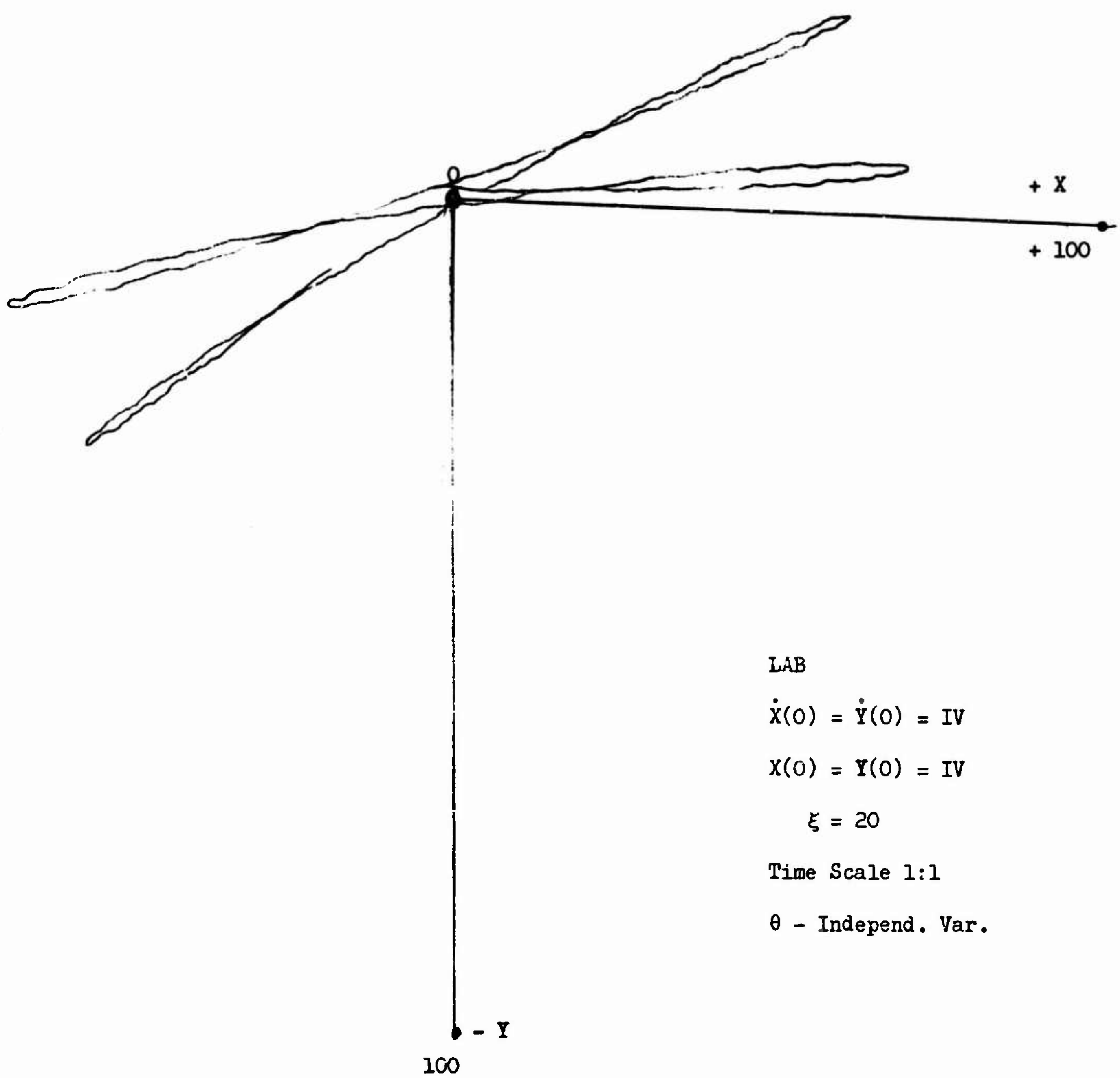
+ X
+ 100
LAB
$\dot{X}(0) = \dot{Y}(0) = IV$
$X(0) = Y(0) = IV$
$\xi = 20$
Time Scale 1:1
θ - Independ. Var.
- Y
100

FIGURE 9.

(i) The Cusped Geometry.*

Particle leakage in the cusped geometry occurs at:

1. the line cusp.

2. the points cusps.

There seems to be two possible schemes for applying the rotating field to the cusped geometry in order to prevent, or at least decrease, leakage:

1. The superposition of a rotating field locally in and parallel to a region which includes the line cusp, and the superposition of a rotating field locally near each point cusp in planes parallel to the line cusp.

2. The superposition of a rotating field parallel to the line cusp throughout the field of the cusped geometry. The point cusps would have to reflect most of the particles that the rotating field forces normal to the rotation in order for the method to be feasable. This would evidently impose a restriction on the ratio of the rotating field to the cusp field.

The system in (1) will now be considered. If a rotating field is applied locally in a region which includes the plane of the line cusp, particles tending to escape through the line cusp will be swept azimuthally against the cusp field lines. Both the reflective properties of the cusp field and the confining properties of the rotating field will confine the particles within the line cusp. Simultaneously, the drift velocity imparted to the particles by the rotating field will move them from the rotating field into the portion of the cusp where the particles are in a confined state until they again approach a cusp.

A local rotating field, it is here proposed, would be applied locally also at a value of Z** between the point cusp and the plane of the line cusp, nearer to the point cusp. Particles which are escaping along lines of force toward the point cusp will be deflected against the cusp field line by the rotating field; but, because of the Z-drift, will sometimes pass beyond the rotating field where they will reflect against the cusp field because of the circular motion which they acquired in the rotating field.

Section VII (b) discusses a method of producing a rotating field which is especially suitable for the cusped geometry and mirror machines.

(ii) The Magnetic Mirror.

The rotating field could be applied to the Magnetic Mirror for the same reason application to the point cusp of the cusped geometry seems possible:

---

* Reference 3.

** See Figure 10.

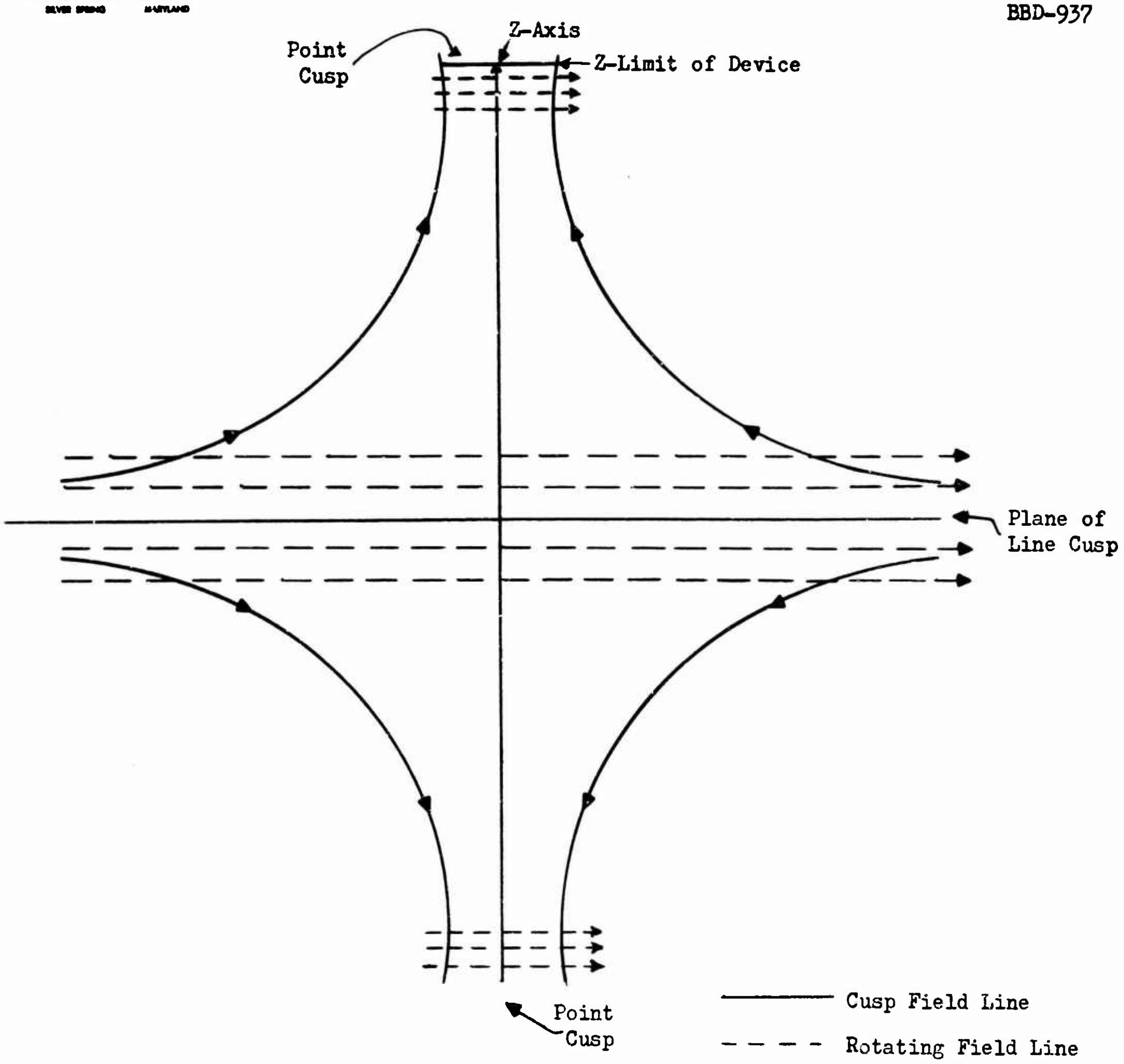

FIGURE 10. The Rotating Magnetic Field Applied Locally to the Cusped Geometry Field.

Particles escaping along lines of force are given azimuthal motion by the rotating field which causes them to reflect from the curved field lines.

A rotating field would be superimposed upon each mirror as shown in Figure 11.

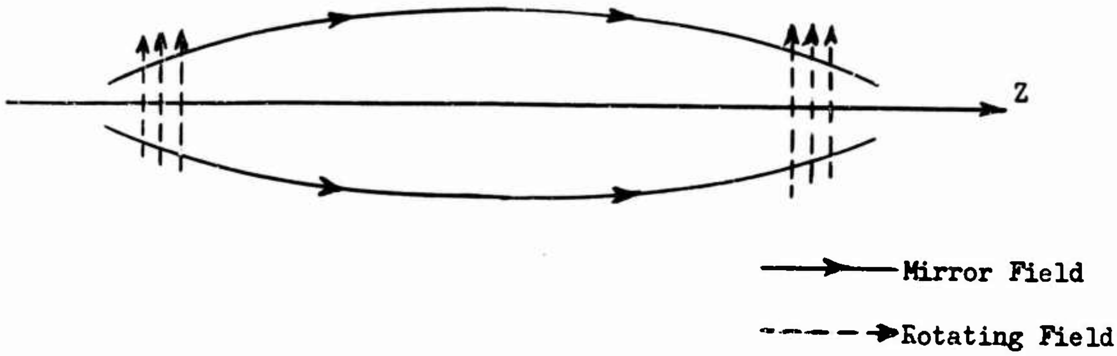

FIGURE 11. The Rotating Magnetic Field Applied Locally to the Magnetic Mirror Field.

(iii) The Stellerator

The property of the rotating magnetic field which makes its application to the stellerator feasibile is the following:

Particles have stable orbits in a rotating magnetic field when $\omega_o > \omega_L$.

The rotating magnetic field would be used as a focusing device in this application to return particles which have drifted from the axis of the stellerator because of the curvature and field gradient drifts which are inherent in the machine. A convenient position for the rotating fields would be on opposite legs of the stellerator as indicated in Figure 12.

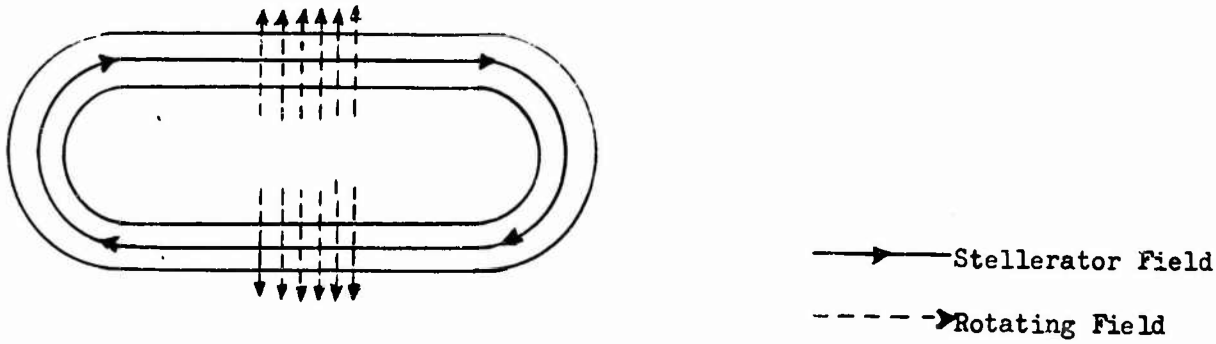

FIGURE 12. The Rotating Magnetic Field Applied Locally to the Stellerator.

VII. Alternate Rotating Fields.

It was shown in Section III that an exactly uniform rotating magnetic field cannot exist. It is in order, therefore, to consider physically possible rotating fields and to note a few of their properties.

(a) Crossed Electromagnetic Field

A rotating magnetic field is formed by (1) the superposition of a plane-polarized EM wave which progresses parallel to the Z-axis upon (2) a plane-polarized EM wave which travels parallel to the y-axis and has the right phase relation with the previous wave. This system of waves will be referred to as a "crossed EM field".

The correct field which fulfills the arbitrality imposed coordinates defined in the previous paragraph is expressed by Equations (43) to (46):

Wave (1)

$$\underline{B}_1 = B_o \sin(\omega_o t - \sigma z)\, \underline{j} \tag{43}$$

$$\underline{E}_1 = E_o \sin(\omega_o t - \sigma z)\, \underline{i} \tag{44}$$

Wave (2)

$$\underline{B}_2 = B_o \cos(\omega_o t - \sigma y)\, \underline{i} \tag{45}$$

$$\underline{E}_2 = E_o \cos(\omega_o t - \sigma y)\, \underline{k} \tag{46}$$

The total field at any point in space is given by

$$\underline{B} = \underline{B_1} + \underline{B_2} \tag{47}$$

$$\underline{E} = \underline{E_1} + \underline{E_2} \tag{48}$$

The result is a non-uniform rotating magnetic field in the xy-plane and a non-uniform rotating electric field in the yz-plane. If σ is small, the field is approximately uniform. For example, if $\omega_o = 3\text{x}10^6$, then $\sigma = 10^{-4}$.

The equations of motion for $\sigma \ll 1$ in coordinates which rotate with the magnetic field were derived as:

$$\ddot{X} + 2\omega_o \dot{Y} - \omega_o^2 X = \omega_L c \sin \omega_o t \cos \omega_o t \tag{49}$$

$$\ddot{Y} - 2\omega_o \dot{X} - \omega_o^2 Y + \omega_L V_Z = \omega_L c \sin^2 \omega_o t \tag{50}$$

$$\ddot{Z} - \omega_L \dot{Y} + \omega_L \omega_o X = \omega_L c \cos \omega_o t \tag{51}$$

The solution of the characteristic determinant (Equation 52) of the associated homogeneous equations gives the result that

$$\begin{vmatrix} D^2 - \omega_o^2 & 2\omega_o D & 0 \\ -2\omega_o D & D^2 - \omega_o^2 & \omega_L D \\ \omega_L \omega_o & -\omega_L D & D^2 \end{vmatrix} = 0 \qquad (52)$$

The Z solution has a component which is again linear in time, which makes one believe that Z-drift must be a fundamental property associated with rotating magnetic fields. The determinant also provides the result that the X and Y and solutions are stable for all ω_o *, unlike the previous case, and the characteristic frequencies are

$$\omega_1 = \sqrt{\omega_o^2 + \omega_L^2} \qquad (53)$$

$$\omega_2 = \omega_o \qquad (54)$$

The inhomogeneous equations can be solved, but this labor has not yet been attempted.

---

* The characteristic determinant has the solution $D^2 = 0$ which implies that there are solutions of the form

$$x = A_1 + B_1\tau$$
$$y = A_2 + B_2\tau$$
$$z = A_3 + B_3\tau,$$

but substitution shows that A_1, B_1, and B_2 are all zero.

(b) Circularly-polarized Electromagnetic Field.

A rotating magnetic field, as well as an RE field, is associated with a circularly-polarized EM field which traverses the Z axis. Such a field, which is self-consistent, is

$$\underline{B} = -\underline{i}\, B_o \cos(\omega_o t - \sigma z) + \underline{j}\, B_o \sin(\omega t - \sigma z) \tag{55}$$

$$\underline{E} = \underline{i}\, E_o \sin(\omega_o t - \sigma z) + \underline{j}\, E_o \cos(\omega t - \sigma z) \tag{56}$$

The equations of motion in laboratory and rotating coordinates are, respectively,

$$m\ddot{x} = qE_o \sin(\omega t - \sigma z) - \frac{V_z B_o}{c} \sin(\omega t - \sigma z) \tag{57}$$

$$m\ddot{y} = qE_o \cos(\omega t - \sigma z) - \frac{V_z B_o}{c} \cos(\omega t - \sigma z) \tag{58}$$

$$m\ddot{z} = \frac{V_x B_o}{c} \sin(\omega t - \sigma z) + \frac{V_y B_o}{c} \cos(\omega t - \sigma z) \tag{59}$$

and

$$\ddot{X} + 2\omega_o \dot{Y} - \omega_o^2 X = -(e - \omega_L V_Z) \sin \sigma Z \tag{60}$$

$$\ddot{Y} - 2\omega_o \dot{X} - \omega_o^2 Y = (e - \omega_L V_Z) \cos \sigma Z \tag{61}$$

$$\ddot{Z} = \omega_L (\dot{Y} - \omega_o X) - (\dot{X} + \omega_o Y) \sin \sigma Z \tag{62}$$

where $e = \frac{qE_o}{m}$

The XY rotation in the Z dimension,

$$\begin{bmatrix} X \\ Y \\ Z \end{bmatrix} = \begin{bmatrix} \cos \sigma Z & \sin \sigma Z & 0 \\ \sin \sigma Z & \cos \sigma Z & 0 \\ 0 & 0 & 1 \end{bmatrix} \begin{bmatrix} \lambda \\ \mu \\ \gamma \end{bmatrix}, \tag{63}$$

removes the sine and cosine coefficients from the equations to give Equations (64) to (66).

$$\ddot{\lambda} + \sigma\mu\ddot{\gamma} + 2\sigma\dot{\mu}\dot{\gamma} - \sigma^2\dot{\gamma}^2\lambda + 2\omega_o\,[-\dot{\mu}+\sigma\lambda\dot{\gamma}] - \omega_o{}^2\lambda = 0 \qquad (64)$$

$$\ddot{\mu} - \sigma\lambda\ddot{\gamma} - 2\sigma\dot{\lambda}\dot{\gamma} - \sigma^2\dot{\gamma}^2\mu + 2\omega_o\,[\dot{\lambda}+\sigma\mu\dot{\gamma}] - \omega_o{}^2\mu = \omega_L\dot{\gamma} - e \qquad (65)$$

$$\ddot{\gamma} + \omega_L\dot{\mu} - \sigma\omega_L\dot{\gamma}\lambda + \omega_L\omega_o\lambda = 0 \qquad (66)$$

No obvious result is immediate except that for small σ, the magnetic field equations, if one replaces $\underline{i}$ by $(-\underline{i})$, reduce to (43) and (45). Thus, one expects the same behavior of the equations of motion for small σ in this case as in the crossed field case.

If interest is generated in regard to particle confinement in crossed fields or circularly-polarized fields, it may be feasible to attempt to solve the equations on the analog computer to check solutions for values of σ other than the limiting one.

It should be noted that the circularly-polarized field has the correct form for producing a rotating field in planes parallel to the line cusp if such a wave is transmitted along the axis of symmetry of a cusped geometry machine.

VIII. Appendices.

Appendix 1. Derivation of the Rotating Field which Reduces to the Given Uniform Field for Small σ.

The equations:

$$\underline{B} = B_o\,[\underline{i}\cos\sigma y\sin\omega_o t + \underline{j}\cos\sigma x\cos\omega_o t] \qquad (A1)$$

$$\underline{E} = -B_o\,[\sin\sigma y\cos\omega_o t + \sin\sigma x\sin\omega_o t]\,\underline{k} \qquad (A2)$$

are derived here by assuming that:

$\underline{B} = B_o\,[\underline{i}\sin\omega_o t + \underline{j}\cos\omega_o t]$ is correct, deriving an expression for $\underline{E}$ by Faraday's law and obtaining a second expression for $\underline{B}$ by Ampere's law. The total field is then equated to the sums of the first and second expressions for $\underline{B}$, and the iteration process is repeated. Additional terms are simultaneously added to $\underline{E}$.

Faraday's law and Ampere's law are, respectively,

$$\underline{\nabla} \times \underline{E} = -\frac{1}{c}\frac{\partial \underline{B}}{\partial t} \qquad \text{and} \qquad (A3)$$

$$\underline{\nabla} \times \underline{B} = \frac{1}{c}\frac{\partial \underline{E}}{\partial t}\,. \qquad (A4)$$

First, assume the field is given by

$$\underline{B}_1 = B_o\,(\underline{i}\sin\omega_o t + \underline{j}\cos\omega_o t) \tag{A5}$$

and substitute $\underline{B}_1$ in (A3), Faraday's law, to obtain the electric field

$$\underline{E} = -\frac{\omega_o B_o}{c}\,[y\cos\omega_o t + x\sin\omega_o t]\,. \tag{A6}$$

Equation (A6) is then substituted in (A4), which gives a second approximation $\underline{B}_2$ to the field $\underline{B}$:

$$\underline{B}_2 = -\frac{\omega_o^2}{2c^2}\,B_o\,[\underline{i}y^2\sin\omega_o t + \underline{j}x^2\cos\omega_o t]\,. \tag{A7}$$

Both $\underline{B}_1$ and $\underline{B}_2$ are approximate solutions to Maxwell's equation [(A3) and (A4)], as $\underline{B}_1 + \underline{B}_2$ is an approximate solution. $\underline{B}_1 + \underline{B}_2$ is substituted back into (A3) to give a new approximation to $\underline{E}$:

$$\underline{E}_2 = -B_o\left[\left(\frac{\omega}{c}y - \frac{\omega_o^3y^3}{3!c^3}\right)\sin\omega_o t - \left(\frac{\omega_o x}{c} - \frac{\omega_o^3x^3}{3!c^3}\right)\cos\omega_o t\right]\underline{k} \tag{A8}$$

If the above process is continued, the fields are represented by the infinite series:

$$\begin{aligned}\underline{B} = B_o\Bigg[&\underline{i}\left(1 - \frac{\omega_o^2y^2}{2!c^2} + \frac{\omega_o^4y^4}{4!c^4} - \frac{\omega_o^6y^6}{6!c^6} + \ldots\right)\sin\omega_o t\\ &+ \underline{j}\left(1 - \frac{\omega_o^2x^2}{2!c^2} + \frac{\omega_o^4x^4}{4!c^4} - \frac{\omega_o^6x^6}{6!c^6} + \ldots\right)\cos\omega_o t\Bigg]\end{aligned} \tag{A9}$$

and

$$\begin{aligned}\underline{E} = -B_o\Bigg[&\left(\frac{\omega_o y}{c} - \frac{\omega_o^3y^3}{3!c^3} + \frac{\omega_o^5y^5}{5!c^5} - \frac{\omega_o^7y^7}{7!c^7} + \ldots\right)\cos\omega_o t\\ &+ \left(\frac{\omega_o x}{c} - \frac{\omega_o^3x^3}{3!c^3} + \frac{\omega_o^5x^5}{5!c^5} - \frac{\omega_o^7x^7}{7!c^7}\right)\sin\omega_o t\Bigg]\hat{k}\end{aligned} \tag{A10}$$

The expressions in parentheses in $\underline{B}$ and $\underline{E}$ converge to sine and cosine respectively, so that Equations (A1) and (A2) are proven to be correct.

Appendix 2. Derivation of Relativistic Fields.

For $\xi = 10$, the velocity of the magnetic field lines approaches the speed of light at about 100 cm if ξ is referenced with respect to conditions for confinement of a deuteron at 100 million degrees. This implies that the situation must be described by relativistic equations for accuracy.

Maxwell's equations, assumed to be Lorentz invariant by the first postulate of special relativity, have the same form in a uniformly translating frame of reference. The Lorentz field transformations are given by*

$$B'_{\parallel} = B_{\parallel} \tag{A11}$$

$$B'_{\perp} = \frac{1}{\sqrt{1-\beta^2}}\left(\underline{B} - \frac{1}{c}\,\underline{V}\times\underline{E}\right)_{\perp} \tag{A12}$$

$$E'_{\parallel} = E_{\parallel}$$

$$E'_{\perp} = \frac{1}{\sqrt{1-\beta^2}}\left(\underline{E} + \frac{1}{c}\,\underline{V}\times\underline{B}\right)_{\perp} \tag{A14}$$

Where $\parallel$ denotes components parallel and $\perp$ components perpendicular to the axis of translation, and $\beta = V/c$.

With the assumption that most of the motion occurs in the $\underline{\theta}$-direction equations (A11) to (A14) are in cylindrical coordinates:

$$B_r' = \frac{1}{\sqrt{1-\beta^2}}\left[B_r - \frac{\omega_o r}{c}\,(\underline{\theta}\times\underline{E})_r\right] \tag{A15}$$

$$B_\theta' = B_\theta \tag{A16}$$

$$B_z' = \frac{1}{\sqrt{1-\beta^2}}\left[B_z - \frac{\omega_o r}{c}\,(\underline{\theta}\times\underline{E})_z\right] \tag{A17}$$

$$E_r' = \frac{1}{\sqrt{1-\beta^2}}\left[E_r + \frac{\omega_o r}{c}\,(\underline{\theta}\times\underline{B})_r\right] \tag{A18}$$

$$E_\theta' = E_\theta \tag{A19}$$

$$E_z' = \frac{1}{\sqrt{1-\beta^2}}\left[E_z + \frac{\omega_o r}{c}\,(\underline{\theta}\times\underline{B})_z\right] \tag{A20}$$

where $\beta = \dfrac{\omega_o r}{c}$.

For simplicity, the low velocity fields are assumed in a rotating frame of reference since it is known the low velocity limit will be taken anyway.

In order to have a uniform rotating field in inertial space, the field in rotating coordinates is the constant B_o and the electric field is zero.

This gives:

$$\left.\begin{aligned} E_r' &= 0 \\ E_\theta' &= 0 \\ E_z' &= 0 \end{aligned}\right\} \qquad (A21)$$

$$\left.\begin{aligned} B_r' &= B_o \sin(\theta - \omega_o t) \\ B_\theta' &= B_o \cos(\theta - \omega_o t) \\ B_z' &= 0 \end{aligned}\right\} \qquad (A22)$$

Combining Equation (A15) to (A22) gives the results:

$$B_r = \frac{B_o \cos(\theta - \omega_o t)}{\sqrt{1-\beta^2}} \qquad (A23)$$

$$B_\theta = B_o \sin(\theta - \omega_o t) \qquad (A24)$$

$$E_z = \frac{\omega_o r B_o \cos(\theta - \omega_o t)}{c\sqrt{1-\beta^2}} \qquad (A25)$$

In the low velocity limit limit (A23) to (A25) reduces to the low velocity limit equations in Section III.

If one sets $\xi = 10$ and $r = 10$, one sees that $\beta = .03$ and

$$\frac{1}{\sqrt{1-\beta^2}} = \frac{1}{\sqrt{.991}} \approx 1,$$

which implies that using the non-relativistic equations gives fairly good accuracy up to this limit of $\omega_o r$.

Appendix 3. Energy Integral.

If the first equation of (12) is multiplied by $\dot{X}$, the second multiplied by Y, the third multiplied by $\dot{Z}$, and the resulting equations are added and integrated; the following conservation law results:

$$\frac{1}{2}\left(\dot{X}^2 + \dot{Y}^2 + \dot{Z}^2\right) - \frac{\omega_o^2}{2}\left(X^2 + Y^2\right) = \text{Constant.}$$

This is the mathematical statement of an interesting property of rotating fields: the kinetic energy with respect to a rotating frame of reference minus the centrifugal potential is constant.

References

1. Electromagnetic Theory, by J. A. Stratton.

2. BBD-848, "Plasma Confinement by a Rotating Magnetic Field", by D. K. Taylor.

3. BBD-869, "Particle Trajections in a Cusped Geometry Magnetic Field", by D. K. Taylor.

THE JOHNS HOPKINS UNIVERSITY
APPLIED PHYSICS LABORATORY
SILVER SPRING MARYLAND

Initial distribution of this document has been made in accordance with a list on file in the Technical Reports Group of the Applied Physics Laboratory, The Johns Hopkins University.